Characterization of Filter Cake Generated by Water-Based Drilling Fluids Using CT Scan

S.M. Elkatatny, SPE, **M.A. Mahmoud,** SPE, and **H.A. Nasr-El-Din,** SPE, Texas A&M University

Summary

Filter-cake characterization is very important in drilling and completion operations. The homogeneity of the filter cake affects the properties of the filtration process such as the volume of filtrate, the thickness of the filter cake, and the best method to remove it. Various models were used to determine the thickness and permeability of the filter cake. Most of these models assumed that the filter cake was homogeneous. The present study shows that the filter cake is not homogeneous, and consists of two layers of different properties.

The objective of this study is to measure the filter-cake thickness and permeability of water-based drilling fluids by a new approach and compare the results with previous models. A high-pressure/high-temperature (HP/HT) filter press was used to perform the filtration process under static conditions (225°F and 300 psi). A computed-tomography (CT) scan was used to measure the thickness and porosity of the filter cake. Scanning electron microscopy (SEM) was used to provide the morphology of the filter cake.

The results obtained from the CT scan showed that the filter cake was heterogeneous and contained two layers with different properties under static and dynamic conditions. Under static conditions, the layer close to the rock surface had a 0.06-in. thickness, 10- to 20-vol% porosity, and 0.087-μd permeability, while under dynamic conditions, this layer had a 0.04-in. thickness, 15-vol% porosity, and 0.068-μd permeability. The layer close to the drilling fluid had a 0.1-in. and 0.07-in. thickness under static and dynamic conditions, respectively, and it had zero porosity and permeability after 30 minutes under static and dynamic conditions. SEM results showed that the two layers contained large and small particles, but there was extremely poor sorting in the layer, that was close to the drilling fluid, which led to zero porosity in this layer. Previous models underestimated the thickness of the filter cake by almost 50%. A new method was developed to measure the thickness of the filter cake, and various models were screened to identify the best model that can predict our permeability measurements.

Introduction

Drilling fluids are a mixture of solids, liquids, and chemicals, with the liquid being the continuous phase. To stabilize the wellbore, the drilling fluid forms a filter cake, which bridges the formation face. Filter cake builds up over the face of the porous medium and filtrate invades the formation (Civan 1994; 1996a, b). When the slurry contains particles of different sizes, the larger particles of the slurry form the skeleton of the filter cake and the smaller particles can migrate and deposit within the porous cake formed by the large particles. Simultaneously, the cake may undergo a compaction process by the effect of the fluid drag as the suspension of smaller particles flows through the cake (Tien et al. 1997).

The filtration process may occur under static or dynamic conditions. Static filtration occurs when the slurry is applied to a filter cake without crossflow. Therefore, the particles are continuously deposited to form thicker filter cakes until the space available is full of the filter cake. Dynamic filtration involves crossflow through the filter cake, which leads to variation in the thickness until the particle deposition and erosion rates become equal (Civan 1998).

At early stages of filtration, both large and small particles deposit on the cake surface; because the drag force driving the particles to the cake surface is high, then only smaller and smaller particles are deposited (Jiao and Sharma 1994). The cake-growth rate gradually decreases until an equilibrium filtration rate is attained at which no particles small enough to be deposited are available in the suspension. This mechanism of cake growth gives rise to a heterogeneous cake with both large and small particles at the internal, and only small particles at the external, portion of the cake.

Permeability of filter cake is controlled by the downhole static and dynamic filtration behavior of the drilling fluid. Thick filter cakes, which have high permeability, cause various operational problems such as excessive torque, drag, high swab and surge pressures, and sticking of pipes. There are many models used to determine the filter-cake permeability. They assume homogeneous filter cake with constant properties of the filter medium.

One approach based on fundamental filtration theory (Tiller 1990, 2002) assumes there is no effect of sedimentation during cake formation. Li et al. (2005) showed a simplified filter-cake permeability-test method based on cake filtration followed by flow through already-formed cake. Rautela (2000) developed an alternative method for determining permeability of the filter cake at the wellsite, where the accuracy is not important. Osisanya and Griffith (1997) developed an equation to determine filter-cake permeability that is based on filtrate volume, shear stress, plastic viscosity, and yield point of the fluid.

The objectives of this work are to (1) characterize filter cake formed from water-based drilling fluids; (2) determine the filter-cake properties such as thickness, porosity, and permeability; and (3) compare laboratory results with available models, that are used to determine the permeability of the filter cake generated by drilling fluids.

Experimental Studies

Materials. Three water-based drilling fluids (A, B, and C) were selected. In Drilling Fluid A, calcium carbonate was used as a weighting material and bentonite was used as a viscosifier **(Table 1).** To increase the density of the previous drilling fluid, the amount of calcium carbonate was increased from 28 to 40 g (Formula B in Table 1). In Formula C, manganese tetraoxide ($d_{50} = 1$ μm) and calcium carbonate **(Table 2)** were used to increase the density of Drilling Fluid A. The mean diameter of calcium carbonate particles, d_{50}, used in the three fluids was 50 μm.

Ceramic disks (10 μm) of 775-md permeability were used to simulate the formation for the filtration process at a desirable temperature and pressure. The initial porosity of the ceramic disk was determined by the difference in weight of the disk in dried and saturated conditions, and it was found to be 38 vol%.

Preparation of Drilling Fluids. The drilling fluid (Drilling Fluid A) was prepared by mixing 319 g of deionized water (base fluid) with 18 g of bentonite, which was used as a filtration control

This paper (SPE 144098) was accepted for presentation at the SPE European Formation Damage Conference, Noordwijk, the Netherlands, 7–10 June 2011, and revised for publication. Original manuscript received for review 3 August 2011. Revised manuscript received for review 22 February 2012. Paper peer approved 27 February 2012.

TABLE 1—LABORATORY FORMULAS TO PREPARE THE EQUIVALENT OF 1 BBL

Additive	Description/Function	Lab Amount (g)	
		Drilling Fluid A	Drilling Fluid B
Water	Base fluid	319	319
Bentonite	Clay for viscosity/API filtrate control	18	18
Carboxymethyl cellulose	API/HP/HT filtrate control	0.25	0.25
Highly oxidized leonardite	API/secondary thinner	4.0	4.0
Caustic soda	Alkali, raise the pH	0.6	0.6
Calcium carbonate ($d_{50} = 50$ μm)	Weight material/bridging agent	28	40
Calcium montmorillonite clay	Weighting material	27	27

TABLE 2—LABORATORY FORMULA TO PREPARE 1 BBL OF DRILLING FLUID C

Additive	Description/Function	Lab Amount (g)
Water	Base fluid	319
Bentonite	Clay for viscosity/API filtrate control	18
Carboxymethylcellulose	API/HP/HT filtrate control	0.25
Highly oxidized leonardite	API/secondary thinner	4.0
Caustic soda	Alkali/raise the pH	0.6
Calcium carbonate ($d_{50} = 50$ μm)	Weight material/bridging agent	28
Calcium montmorillonite clay	Simulated solids	27
Manganese tetra oxide ($d_{50} = 1$ μm)	Weighting material	50

TABLE 3—PROPERTIES OF DRILLING FLUIDS A AND B

Property	Conditions	Units	Value	
			Drilling Fluid A	Drilling Fluid B
Density	75°F and 14.7 psi	ppg	9.2	9.6
Plastic viscosity	120°F and 14.7 psi	cp	12	12
Yield point	120°F and 14.7 psi	lb/100 ft^2	8	7
10-s gel strength	120°F and 14.7 psi	lb/100 ft^2	4	3
10-s gel strength	120°F and 14.7 psi	lb/100 ft^2	10	10
pH	75°F and 14.7 psi	–	8.9	8.9

agent, for 20 minutes. 0.25 g of sodium carboxymethyl cellulose, which was used as an HP/HT filtrate control agent, was added and mixed for 5 minutes. 4.0 g of highly oxidized leonardite, which was used as a thinner, was added with 0.6 g of caustic soda, which was used as an alkalinity agent, and they were mixed for 5 minutes. 28 g of calcium carbonate, which was used as a weighting and bridging material, was added and mixed for 10 minutes. Finally, 27 g of altered calcium montmorillonite clay, which was used as a simulated fluid, was added and mixed for 5 minutes. Drilling Fluid B was prepared in a similar procedure; however, 40 g of $CaCO_3$ was used. Drilling Fluid C was prepared by adding 50 g of manganese tetraoxide to Drilling Fluid A after calcium montmorillonite clay and mixing for 20 minutes.

TABLE 4—PROPERTIES OF DRILLING FLUID C

Property	Condition	Units	Value
Density	75°F and 14.7 psi	ppg	10.3
Plastic viscosity	120°F and 14.7 psi	cp	13
Yield point	120°F and 14.7 psi	lb/100 ft^2	11
10 s gel strength	120°F and 14.7 psi	lb/100 ft^2	4
10 s gel strength	120°F and 14.7 psi	lb/100 ft^2	10
pH	75°F and 14.7 psi	–	8.7

Properties of Drilling Fluids. **Table 3** summarizes the properties of Drilling Fluids A and B. The fluid properties were measured by using mud balance and a Fann 35 viscometer. The results obtained were 9.2 ppg for density of 28 g $CaCO_3$ and 9.6 ppg for 40 g $CaCO_3$, 12 cp for a plastic viscosity measured at 120°F, 8 lbf/100 ft^2 for a yield point, and pH of 8.9. **Table 4** shows that the density can be increased to 10.3 ppg by using manganese tetraoxide, and that the rheological properties of the drilling fluids were stable, as compared with Drilling Fluids A and B. No phase separation was recorded for Drilling Fluids A and C, even after 16 hours under hot rolling.

Table 5 summarizes the results of the sieve analysis performed on the solid components presented in the three drilling fluids. **Fig. 1** gives the d_{50} of the different drilling fluids. Drilling Fluid C had d_{50} greater than Drilling Fluids A and B, which means fewer fine particles.

Results and Discussion

HP/HT Filtration. Drilling Fluids A, B, and C were put in the HP/HT cell at 300-psi differential pressure and 225°F. The filtrate

TABLE 5—SIEVE ANALYSIS OF DIFFERENT SOLIDS USED TO PREPARE DRILLING FLUIDS A, B, AND C

		Drilling Fluid A		Drilling Fluid B		Drilling Fluid C	
Sieve Number	Sieve Size (mm)	Retained Weight (%)	Cumulative Weight (%)	Retained Weight (%)	Cumulative Weight (%)	Retained Weight (%)	Cumulative Weight (%)
20	> 0.85	0.14	0.14	0.17	0.17	6.34	6.34
30	0.85–0.6	0.12	0.26	0.14	0.31	3.20	9.53
40	0.6–0.425	0.19	0.45	0.22	0.53	5.13	14.66
50	0.425–0.3	0.57	1.01	0.56	1.09	5.86	20.52
70	0.3–0.212	2.20	3.22	2.35	3.44	6.90	27.42
100	0.212–0.15	4.31	7.53	5.15	8.60	5.21	32.63
140	0.15–0.106	6.83	14.35	7.77	16.37	6.32	38.95
170	0.106–0.09	4.92	19.27	4.86	21.22	5.37	44.31
200	0.09–0.075	6.00	25.27	26.66	47.89	21.69	66.01
325	0.075–0.045	25.21	50.48	14.78	62.67	15.38	81.39
Pan	< 0.04	49.52	100.00	37.33	100.00	18.61	100.00

volume was measured as a function of time for 30 minutes, and the results are shown in **Fig. 2. Table 6** summarizes the results of the spurt volume and the filtrate volume of each drilling fluid. Drilling Fluid A gave the highest spurt volume 4.3 cm^3. The spurt volume decreased as the amount of calcium carbonate was increased, as in Drilling Fluid B.

CT Scan. The filter cake that formed from Drilling Fluid A was scanned twice in wet and dry conditions. In the wet case, two layers were observed with different thicknesses and CT numbers (CTNs). The CTN for the layer close to the surface of the disk and that for the layer close to the drilling fluid were 1,500 and 500, respectively. The filter cake was dried at 250°F for 3 hours, and the CTN was 1,200 for the layer close to the rock surface and 500 for the layer close to the drilling fluid. The experiment was repeated four times to confirm the results obtained, as shown in **Figs. 3 and 4. Fig. 5** shows that the filter cake contained the two layers even with an increase in the density of the drilling fluid to 9.6 ppg (Drilling Fluid B). The presence of two layers was also confirmed by using manganese tetraoxide, as shown in **Fig. 6.**

The filter disk was scanned before the experiment in wet and dry conditions to determine the initial porosity. The CTNs for wet and dry conditions were 1,550 and 1,180, respectively. The initial porosity of the disk was calculated from these readings and was found to be 37 vol%.

In the following sections, the filter cake formed by using Drilling Fluid A was selected for detailed analysis. The filtrate-fluid density for Formula A was measured using a high-temperature density meter (DMA 4100) at different temperatures, as shown in **Fig. 7,** and the kinematic viscosity was obtained using a capillary-tube viscometer (Ubbelhold type). The viscosity of the cumulative filtrate was 0.2 cp at 225°F, as shown in **Fig. 8.**

SEM. The SEM scan was performed on the filter cake to determine the morphology of each layer. It was noticed that there was a difference in the particle-size distribution in each layer, as shown in **Fig. 9.** Grain size was measured using a Leica microscope. The obtained results showed that the layer close to the surface of the disk contained grains of a large size, in the range of

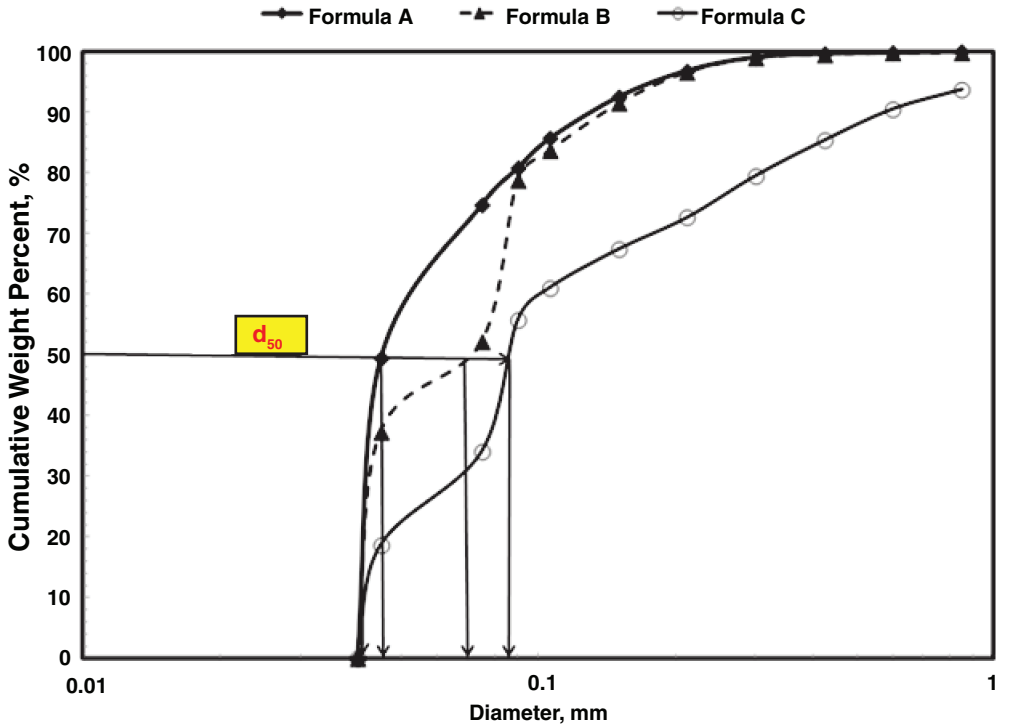

Fig. 1—Particle-size distribution of drilling solids used to prepare the three drilling fluids.

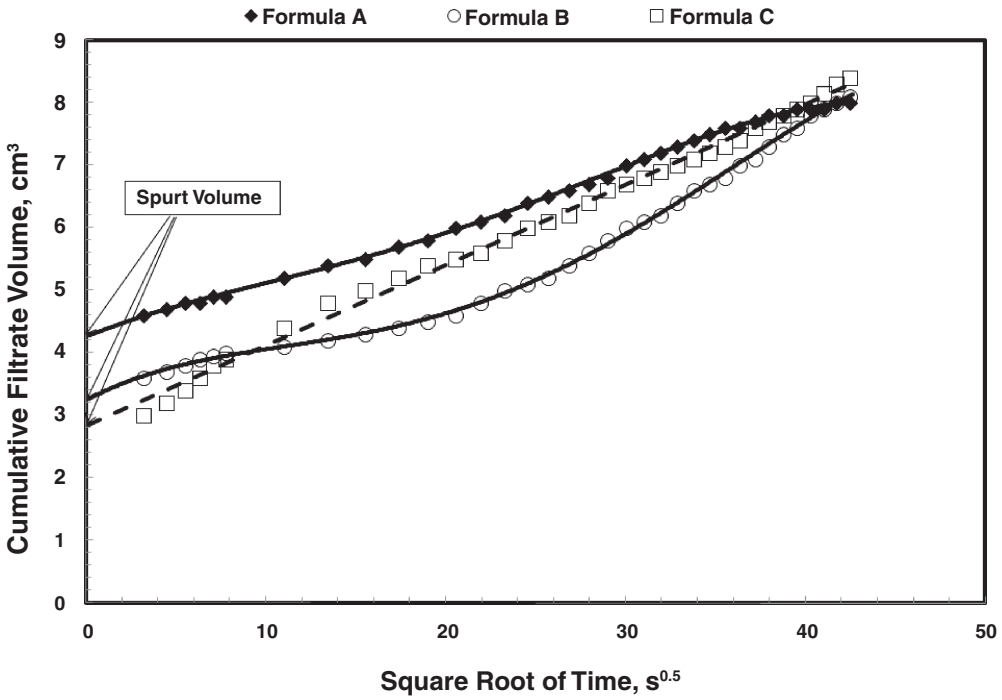

Fig. 2—Cumulative filtrate volume as a function of the square root of time for Drilling Fluids A, B, and C.

TABLE 6—RESULTS OF HP/HT FILTER PRESS FOR THE THREE DRILLING FLUIDS

Drilling Fluid	Spurt Volume (cm^3)	Cumulative Filtrate Volume after 30 min (cm^3)
A	4.3	8
B	3.2	8.1
C	2.8	8.4

160–280 μm, and that the layer close to the drilling fluid contained a mixture of grains of both small size in the range of 90–100 μm and large size in the range of 150–260 μm **(Fig. 10).**

Reaction With HCl. A dilute HCl solution (0.1 M) was prepared from concentrated HCl (36.5-wt% ACS reagent grade) using deionized water with a resistivity of 18.2 MΩ.cm at room temperature. The filter cake was dried at 300°F for 3 hours. The two layers were separated. HCl was added to each layer and images were taken before and after adding the acid **(Fig. 11).**

After adding HCl, a rapid reaction within the layer close to the surface of the disk with evolving bubbles was noticed. The reaction of the layer close to the drilling fluid, however, was much slower. The top of the layer close to the drilling fluid did not respond to the acid, while the bottom of this layer showed weak dissolution. The two layers were imaged after the reaction, as shown in **Fig. 12.** The rapid reaction with the evolving bubbles is an indication that the constitute of the layer close to the rock surface was mainly calcium carbonate, which existed only in the lower part of the layer close to the drilling fluid that showed the same type of dissolution.

Porosity Determination. The porosity of each layer of the filter cake and the disk was obtained from CT scan using Eq. 1:

$$\phi = \frac{CT_{wet} - CT_{dry}}{CT_{water} - CT_{air}}, \quad \ldots\ldots\ldots\ldots\ldots\ldots\ldots\ldots\ldots\ldots (1)$$

where CT_{wet} = CTN of the porous medium saturated with water, CT_{dry} = CTN of the porous medium when dry, CT_{water} = CTN of water (0.0), and CT_{air} = CTN of air (–1,000).

The CTN for the layer close to the drilling fluid in wet conditions was equal to the CTN of this layer in dry conditions. This means that the porosity of the layer close to the drilling fluid was zero. It was observed that the porosity of the layer close to the rock surface ranged from 10 to 20 vol% **(Table 7).**

The porosity of the disk was calculated using Eq. 1. Before the filtration process, the porosity of the ceramic disk was found to be 37 vol%, while after the filtration process, it was in the range of 20 to 25 vol%. The change in the porosity of the filter disk indicates a decrease in its permeability, which should be considered when calculating the permeability of the filter cake.

Calculation of Filter-Cake Thickness. Table 7 gives the thickness for each layer. The thickness of the layer close to the drilling fluid was 0.09 to 0.1 in. It was greater than the thickness of the layer close to the surface of the disk, which was 0.05 to 0.07 in.

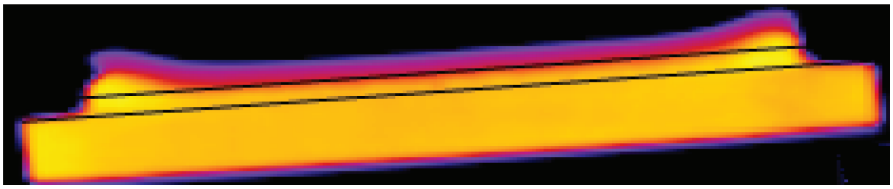

Fig. 3—Filter-cake heterogeneity as shown by the 2D CT scan: Drilling Fluid A.

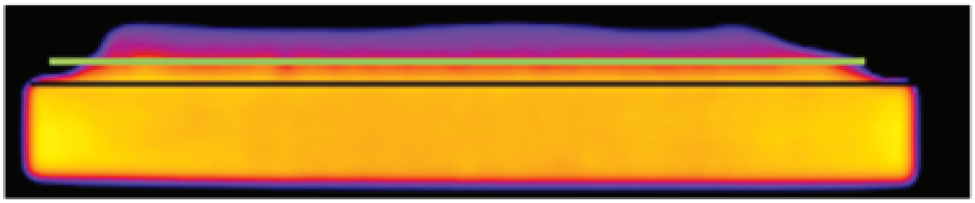

(a) Second Experiment - Drilling Fluid A.

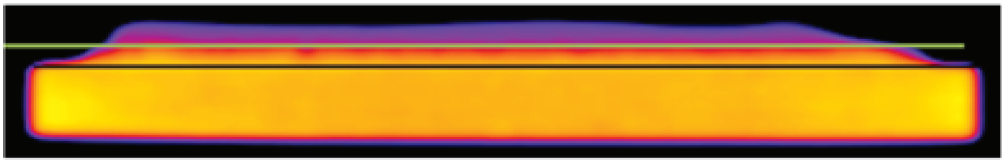

(b) Third Experiment – Drilling Fluid A.

Fig. 4—Drilling fluid (Formula A) was prepared several times. Filter cake [(a) and (b)] always contained two layers.

Fig. 5—Filter-cake layers of the drilling fluid of 9.6 ppg.

The thickness of the filter cake, L_c, can be determined using different models. Bourgoyne et al. (1991) and Tiller (2002) used the same model to calculate L_c (Eq. 2):

$$L_c = \frac{1}{\left(\frac{\varepsilon_{sav}}{\phi_s} - 1\right)} * \frac{V_f}{A}, \quad \ldots\ldots\ldots\ldots\ldots\ldots\ldots\ldots (2)$$

where A = area of the filter disk (cm^2), L_c = thickness of filter cake (cm), V_f = filtrate volume (cm^3), ε_{sav} = volume fraction of the solids in the cake, and ϕ_s = volume fraction of the solids in the drilling fluid.

Khatib (1994) provided an empirical relationship of $CaCO_3$ filter cake of 25 to 35 vol% porosity to obtain the thickness of the filter cake (Eq. 3):

$$L_c = \frac{w * \rho_L}{\rho_s(1 - \phi_c)} * \frac{V_f}{A}, \quad \ldots\ldots\ldots\ldots\ldots\ldots\ldots\ldots (3)$$

where A = area of the filter disk (m^2); L_c = thickness of the filter cake (cm); V_f = filtrate volume (m^3); w = mass fraction of solids in the drilling fluid, ρ_L = density of the drilling fluid, kg/m^3; ρ_s = density of solids, kg/m^3; and ϕ_c = porosity of the filter cake.

The volume fraction of solids in mud (ϕ_s) was 0.09, and the volume fraction of solids in the cake (ε_{sav}) was 0.33. **Table 8** gives the thickness of the filter cake for the models mentioned previously. The six models underestimated the thickness of the filter cake by almost 50%. These models consider the filter cake as one layer, which is not the case. As a result, the model predictions are not accurate, as shown in Tables 7 and 8.

Determination of the Permeability of the Filter Cake. Permeability of the filter cake was obtained using different models. Bourgoyne et al. (1991) (Eq. 4) calculated the permeability under static condition from the relationship between the cumulative filtrate volume and the square root of time, as shown in Fig. 2.

$$V_f = \sqrt{2k_c\Delta p\left(\frac{\varepsilon_{sav}}{\phi_s} - 1\right)A\frac{\sqrt{t}}{\sqrt{\mu}}}, \quad \ldots\ldots\ldots\ldots\ldots\ldots (4)$$

where A = area of the filter disk (cm^2), k_c = permeability of the mud cake (darcy), t = time of filtration, V_f = filtrate volume (cm^3), Δp = pressure drop across the mud cake, μ = viscosity of the filtrate, ε_{sav} = volume fraction of the solids in the cake, and ϕ_s = volume fraction of the solids in the drilling fluid.

Khatib (1994) provided an empirical relationship of $CaCO_3$ filter cake of 25 to 35 vol% porosity to obtain the permeability (Eq. 5):

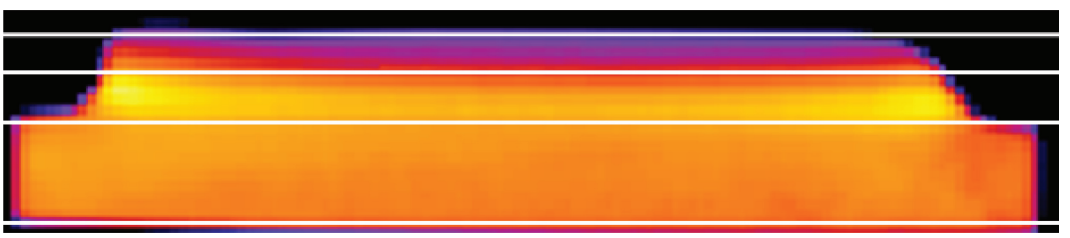

Fig. 6—Filter-cake layers of Drilling Fluid C with 10.3 ppg.

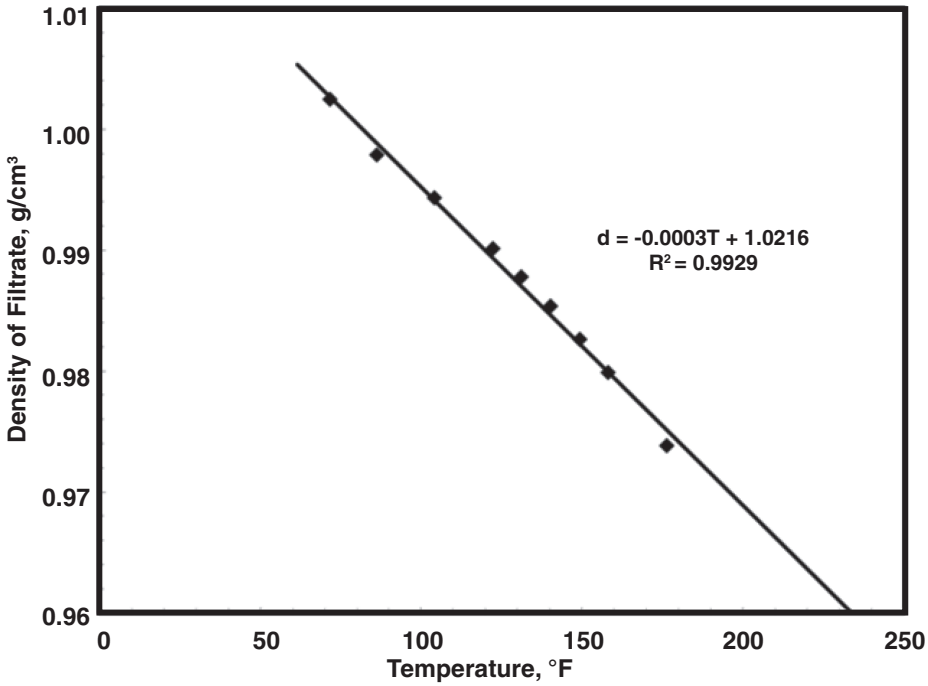

Fig. 7—Density of filtrate as a function of temperature for Drilling Fluid A.

$$k_c = 112.7 * e^{-8.8(1-\phi_c)}, \quad \ldots\ldots\ldots\ldots\ldots\ldots\ldots\ldots (5)$$

where k_c = permeability of the filter cake (md) and ϕ_c = porosity of the filter cake.

When the accuracy is not of prior importance, the permeability can be determined by an empirical correlation developed by Rautela (2000) (Eq. 6):

$$k_c = Q_w * Q_c * 1.99 \times 10^{-3}, \quad \ldots\ldots\ldots\ldots\ldots\ldots\ldots\ldots (6)$$

where k_c = permeability of the filter cake (m^2), Q_w = filtrate volume, and Q_c = volume of the filter cake.

Tiller (2002) gave a procedure to calculate the permeability of the filter cake (Eqs. 7 through 9):

$$c = \phi_s/(1 - \phi_s/\varepsilon_{sav}), \quad \ldots\ldots\ldots\ldots\ldots\ldots\ldots\ldots (7)$$

$$\frac{pdt}{\mu dv} = \alpha_{av} * c * v + R_m, \quad \ldots\ldots\ldots\ldots\ldots\ldots\ldots\ldots (8)$$

$$\alpha_{av} * k_c * \varepsilon_{sav} = 1, \quad \ldots\ldots\ldots\ldots\ldots\ldots\ldots\ldots (9)$$

where k_c = permeability of the filter cake, p = differential pressure, R_m = resistance of the filter medium, t = time, v = volume of filtrate per unit area (m), α_{av} = average specific cake resistance,

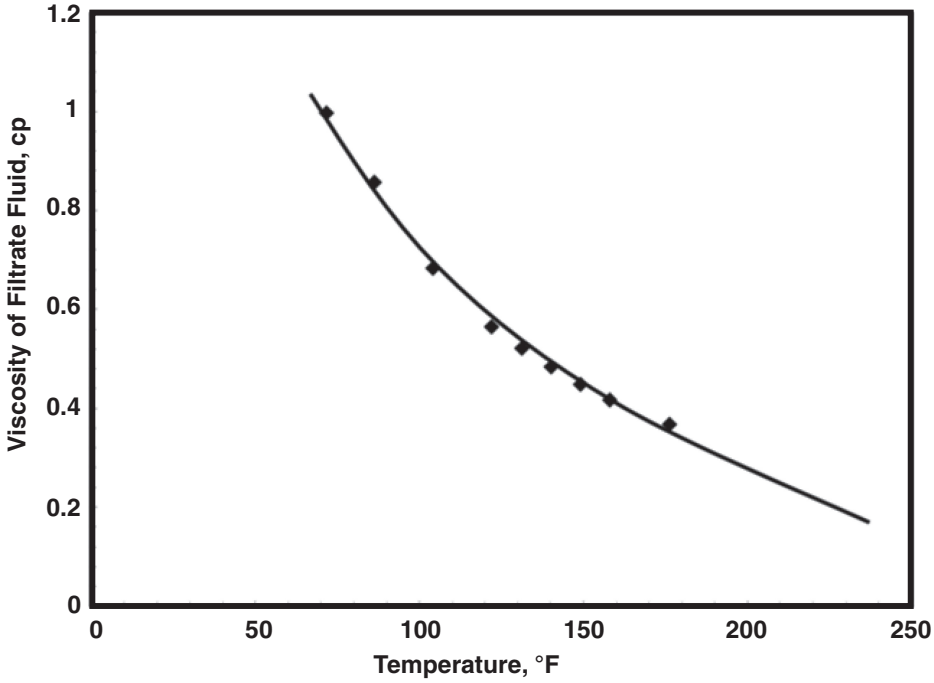

Fig. 8—Viscosity of filtrate as a function of temperature for Drilling Fluid A.

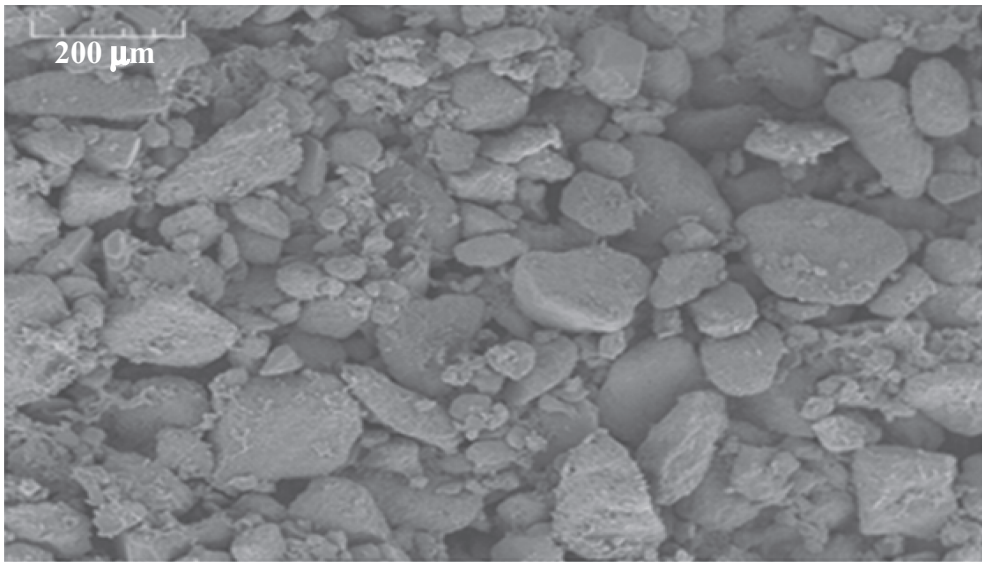

Fig. 9—SEM photomicrograph for both layers. The layer close to the rock surface contained large particles, while there was an extremely poor sorting in the layer close to the drilling fluid.

ε_{sav} = volume fraction of solids in the filter cake, μ = filtrate viscosity, and ϕ_s = volume fraction of solids in the drilling fluid.

The average specific cake resistance (α_{av} 6×10^{19} 1/m^2) was obtained from the slope of the line shown in **Fig. 13** and used to calculate the permeability using Eq. 9.

Martinez et al. (2000) developed another method to calculate the permeability, as shown in **Fig. 14—**the slope of Eq. 10 is equal to 1/ ($2k_C$).

$$\frac{pt}{\mu v} = \left(\frac{1}{2k_c}\right)L_c + R_m, \quad \ldots\ldots\ldots\ldots\ldots\ldots\ldots\ldots (10)$$

where k_c = permeability of the filter cake (m^2), L_c = cake thickness (m), p = filtration pressure, R_m = medium resistance, t = time, v = filtrate volume per unit area (m^3/m^2), and μ = viscosity of filtrate.

The Li et al. (2005) method, which depends on the relationship between the cumulative filtrate volume and time as shown in **Fig. 15,** can be used to obtain the filter-cake permeability. The slope is equal to the flow rate (0.0015 cm^3/s = 5.86×10^{-7} m^3/m^2–s), from which the pressure drop across both the filter medium and filter cake can be obtained using Eq. 11. The pressure drop across the filter cake can be obtained from Eq. 12; then, the filter-cake permeability can be determined from Eq.13.

$$q = k_m \frac{\Delta P_m}{\mu L_m}, \quad \ldots\ldots\ldots\ldots\ldots\ldots\ldots\ldots (11)$$

$$\Delta P_t = \Delta P_m + \Delta P_c, \quad \ldots\ldots\ldots\ldots\ldots\ldots\ldots\ldots (12)$$

$$q = k_c \frac{\Delta P_c}{\mu L_c}, \quad \ldots\ldots\ldots\ldots\ldots\ldots\ldots\ldots (13)$$

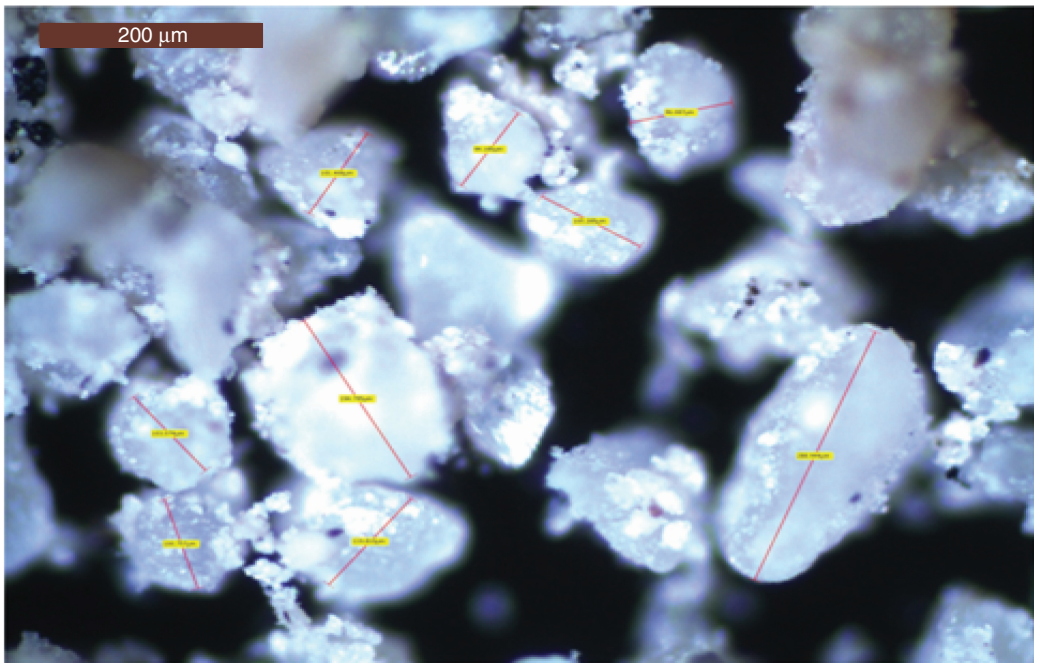

Layer close to drilling fluid

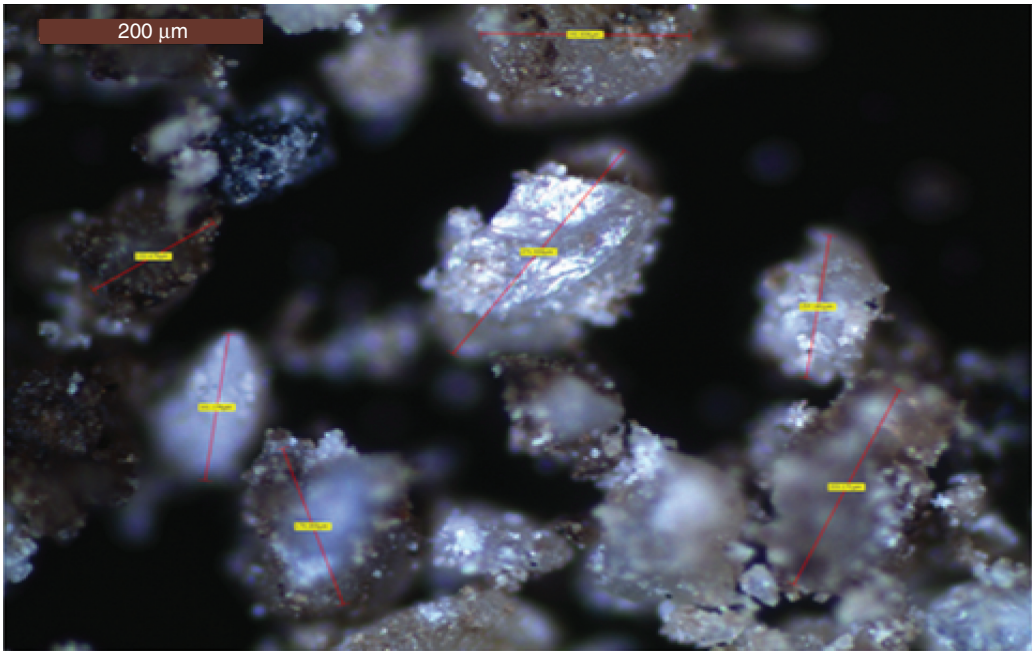

Layer close to rock surface

Fig. 10—Particle size in the layer close to the rock surface ranged from 160–280 μm, while the layer close to the drilling fluid contained small particles (90–100 μm) and large particles (150–260 μm).

where k_c = filter-cake permeability (m^2), k_m = filter-medium permeability, L_c = thickness of filter cake (m), L_m = thickness of the filter medium, q = filtrate rate, μ = filtrate viscosity, ΔP_c = pressure drop across the filter cake, ΔP_m = pressure drop across the filter medium, and ΔP_t = total pressure drop.

For permeability calculation, the models provided by Bourgoyne et al. (1991), Martinez at al. (2000), and Tiller (2002) gave similar results. The Li et al. (2005) model overestimated the permeability because the total thickness of the filter cake was considered, whereas the change in the filter medium was neglected. The Khatib (1994) model, which assumed a homogeneous filter cake, resulted in a higher porosity, which also led to permeabilities higher than the measured ones. The Rautela (2000) model showed inaccurate results because it was applied only in case of negligible accuracy.

The change in the permeability of the filter medium can be obtained from Eq. 14, developed by Lambert (1981). From the

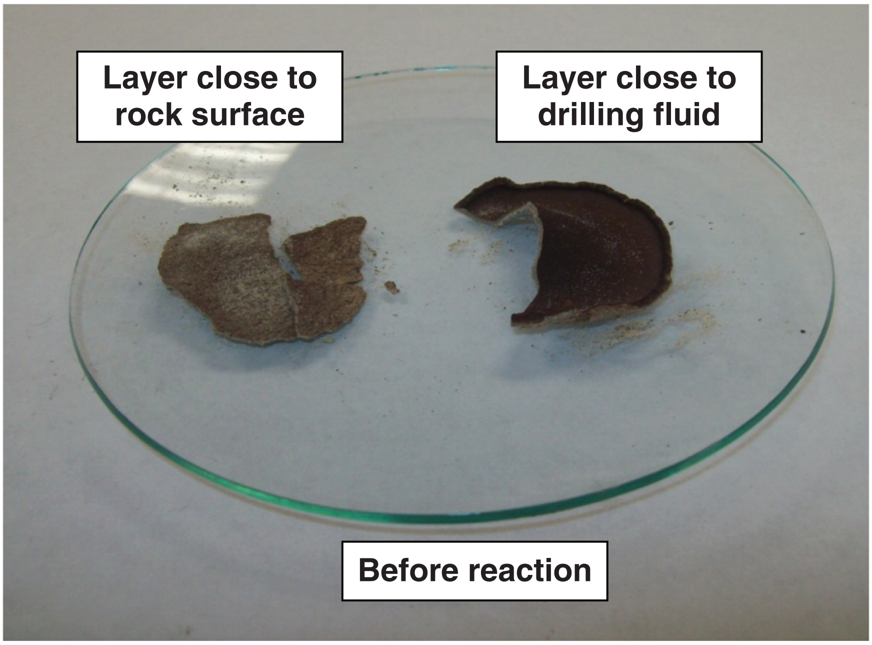

Fig. 11—Segments of the layer close to the rock surface (left) and the layer close to the drilling fluid (right) of the filter cake before reaction with 0.1-M HCl.

CT-scan experiment, the initial porosity was 37 vol% and the final porosity was 20–25 vol%.

$$\frac{k_{\text{final}}}{k_{\text{initial}}} = \left(\frac{\phi_f}{\phi_i}\right)^3, \quad (14)$$

where k_{initial} = initial permeability of the ceramic disk, k_{final} = permeability of the ceramic disk after filtration process, ϕ_i = initial porosity of ceramic disk, and ϕ_f = final porosity of ceramic disk after filtration process.

From Eq. 14, the final permeability of the ceramic disk ($\phi_f = 0.20$) was estimated to be 122 md. Using the Li et al. (2005) method (Eqs. 11 through 13) with the thickness of the filter cake being equal to the thickness of the layer close to the rock surface only, and the final permeability of the filter medium, the permeability of the layer close to the rock surface becomes 0.087 μd, which is comparable with the models developed by Bourgoyne et al. (1991), Martinez et al. (2000), and Tiller (2002).

Permeability calculations using different models [Bourgoyne (1991) and Tiller (2002)] depend on the value of the calculated filter-cake thickness (Eqs. 2 and 3). Therefore, the inaccuracy of the filter-cake thickness, which was proved in this study, will result in incorrect filter-cake permeability. The Li et al. (2005) model consists of simple equations, in which the filter-cake thickness and

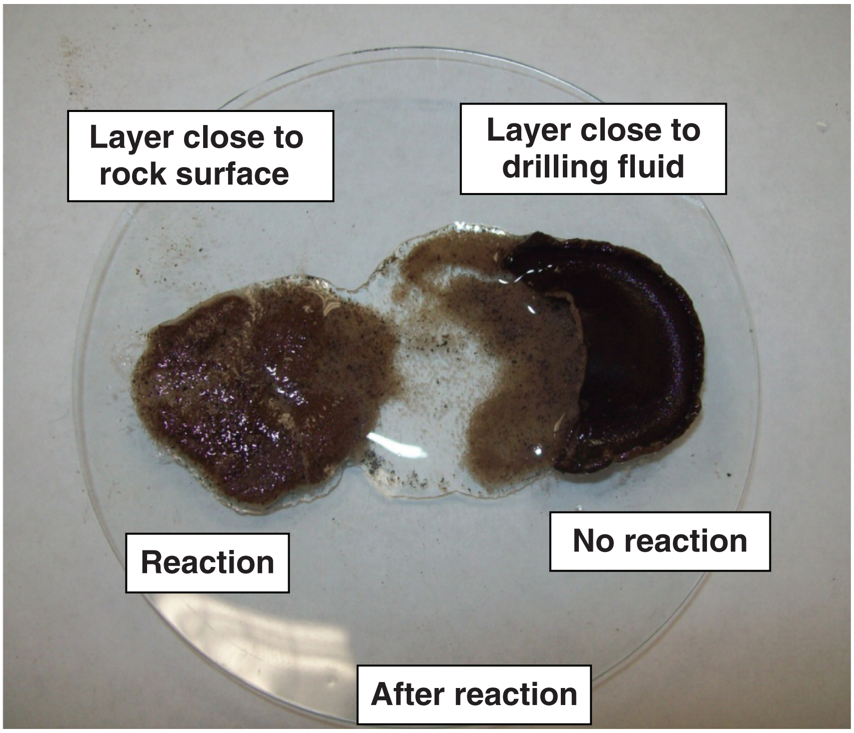

Fig. 12—Complete dissolution of the layer close to the rock surface (left) and partial dissolution of the layer close to the drilling fluid (right) of the filter cake after reaction with 0.1-M HCl.

TABLE 7—CALCULATION OF THE PROPERTIES OF THE FILTER CAKE AND THE FILTER DISK BY USE OF CT SCAN AT THE END OF EXPERIMENT

	Layer Close to the Drilling Fluid		Layer Close to the Surface of the Disk		
Experiment	Thickness (in.)	Porosity (vol%)	Thickness (in.)	Porosity (vol%)	Filter-Disk Porosity (vol%)
1	0.1	Zero	0.07	20	20
2	0.08	Zero	0,06	10	20
3	0.1	Zero	0.07	15	25
4	0.09	Zero	0.05	10	25

TABLE 8—PREDICTION OF THE TOTAL FILTER-CAKE THICKNESS AND PERMEABILITY USING DIFFERENT MODELS (EQS. 3 THROUGH 11)

Model	Permeability (μd)	Filter Cake Thickness (in.)
Bourgoyne (1991)	0.023	0.045
Martinez et al. (2000)	0.050	0.045
Tiller (2002)	0.050	0.045
Li et al. (2005)	0.189	0.17
Khatib (1994)	63	0.0127
Rautela (2000)	170	–

the filtrate rate are inputs. The thickness in this method was accurate because it was measured by caliper or by using software. Also, this model takes into consideration the change in filter-medium properties, which was ignored by other models.

Therefore, it can be concluded that the Li et al. (2005) method is the simplest way for determination of the filter cake permeability. This method depends on the fluid flow through already-formed filter cake and displays simple and more-accurate calculations of filter-cake permeability.

Dynamic Filtration Results. HP/HT filtration tests were performed for a 9.2-ppg drilling fluid under dynamic conditions (100 rpm). The test was performed at 225°F and 300-psi differential pressure. **Fig. 16** shows that the formed filter cake was heterogeneous under dynamic conditions, with a layer close to the drilling fluid (0.07 in.) and a layer close to the rock surface (0.04 in.). It was noticed that the thickness of both layers was less than the thickness of these layers under static conditions. This was because of the forces that affect the solid particles under dynamic conditions (Al-Abduwani et al. 2005).

The average CTNs of the layer close to the surface of the disk in wet and dry conditions were 1,100 and 950, respectively. Using Eq. 1, the porosity for this layer was 15 vol%. The average CTN for the layer close to the drilling fluid was 500 and 650 in wet and dry conditions, respectively, which give zero porosity for this layer after 30 minutes of filtration. The value of the porosity of both layers was in the same range under static and dynamic conditions.

Fig. 17 shows the cumulative filtrate volume as a function of time under dynamic conditions. The slope q was 0.0018 cm^3/s (7.031×10^{-7} m^3/m^2–s), and by applying the Li et al. (2005) method, the permeability of the layer close to the rock surface was equal to 0.068 μd, which was smaller than the permeability of this layer under static conditions.

Conclusions

The characteristics of filter cake formed by water-based drilling fluids were measured by use of CT scan. Various models to predict thickness and permeability of the filter cake were examined.

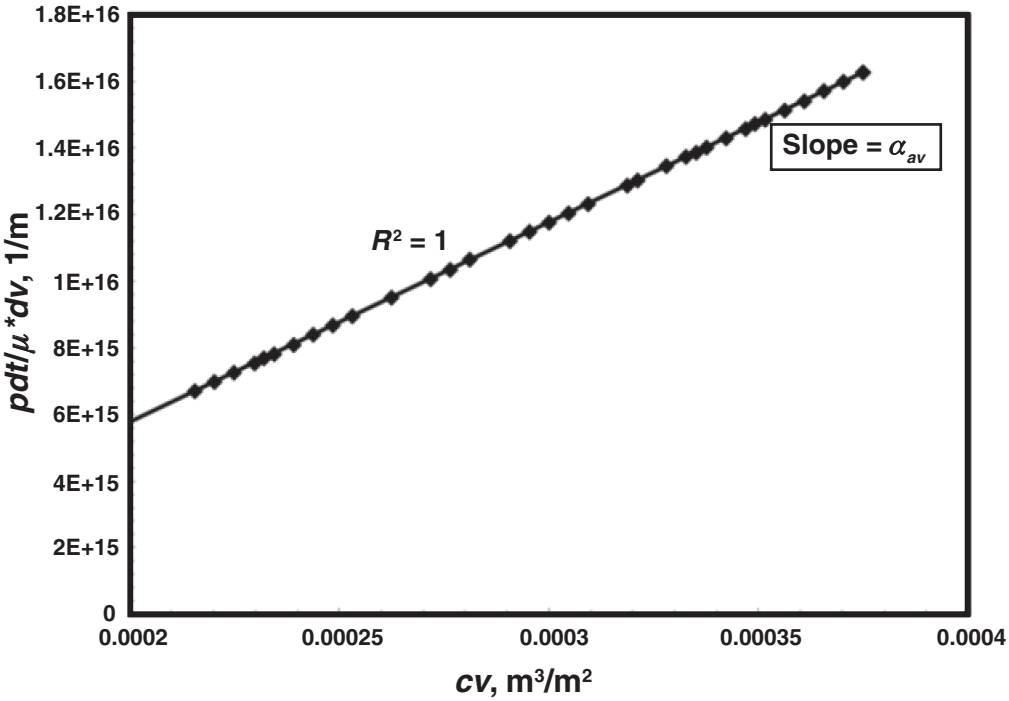

Fig. 13—Tiller (2002) method used to determine the permeability of the filter cake.

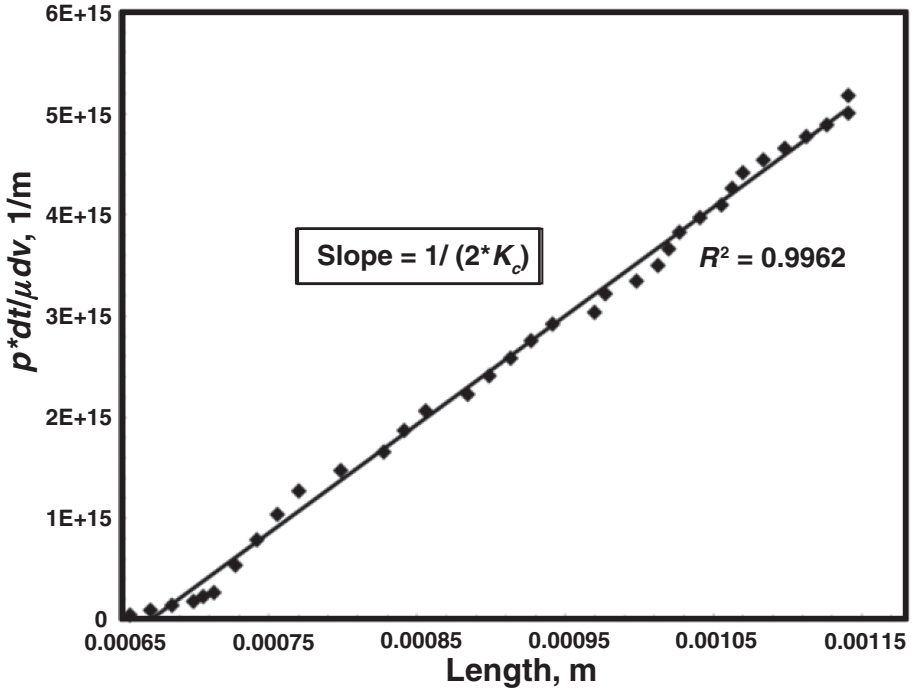

Fig. 14—Martinez et al. (2000) method used to determine the permeability of the filter cake.

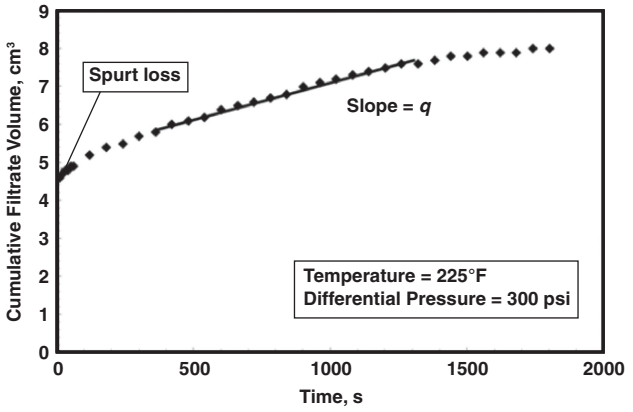

Fig. 15—Li et al. (2005) method used to determine the permeability of the filter cake.

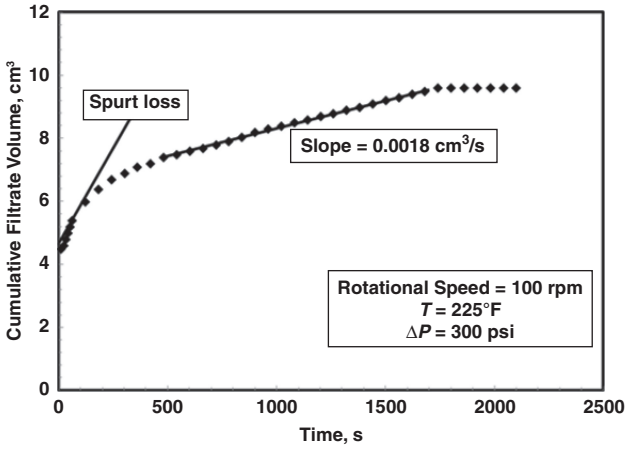

Fig. 17—Cumulative filtrate volume as a function of time of Drilling Fluid A under dynamic conditions (100 rpm).

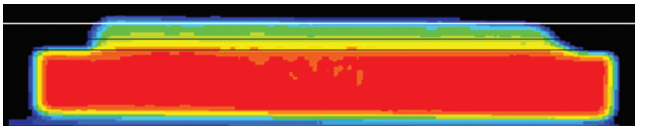

Fig. 16—Heterogeneity of the filter cake of Drilling Fluid A under dynamic conditions (100 rpm).

On the basis of the results obtained, the following conclusions can be made:

1. The filter cake was heterogeneous, with two distinct layers having different properties. The two layers were clearly noted under static and dynamic conditions.
2. The filter cake was thinner and had a lower permeability under dynamic conditions than was the case under static conditions.
3. The layer close to the drilling fluid was thicker than the layer close to the surface of the disk. The porosity in the layer close to the drilling fluid was zero, while the porosity of the layer close to the rock surface was found to be in the range of 10 to 20 vol%, under static and dynamic conditions.
4. The layer close to the surface of the disk consisted mainly of calcium carbonate, while the layer close to the drilling fluid contained the rest of the drilling solids used in Drilling Fluid A under static and dynamic conditions.
5. A CT scanner is a good tool to determine the thickness and porosity of the filter cake. It also provided the change in the porosity and permeability of the ceramic disk, which should be considered in the calculation of the filter-cake permeability.
6. Previous models treated the filter cake as a single homogeneous layer, which adversely affected model predictions of thickness and permeability of the filter cake.
7. Permeability predictions using the method of Li et al. (2005) were in good agreement with the experimental results obtained in the present study.

Nomenclature

A = area of the filter disk
CT_{air} = CTN of air (–1,000)
CT_{dry} = CTN of the porous medium when dry

CT_{water} = CTN of water (0.0)
CT_{wet} = CTN of the porous medium when saturated with water
k_c = permeability of the mudcake
$k_{initial}$ = initial permeability of the ceramic disk, md
k_{final} = permeability of the ceramic disk after filtration process, md
K_c = filter-cake permeability, m^2
K_m = filter-medium permeability, m^2
L_c = thickness of filter cake
L_m = thickness of filter medium, m
p = filtration pressure, Pa
P = differential pressure, Pa
q = filtrate rate, $m^3/m^2.s$
Q_c = volume of the filter cake, cm^3
Q_w = filtrate volume, cm^3
R_m = resistance of the filter medium, 1/m
t = time of filtration, seconds
v = filtrate volume per unit area
w = mass fraction of solids in the drilling fluid
V_f = filtrate volume
α_{av} = average specific cake resistance, $1/m^2$
Δp = pressure drop across the mud cake, atm
ΔP_c = pressure drop across the filter cake, Pa
ΔP_m = pressure drop across the filter medium, Pa
ΔP_t = total pressure drop, Pa
ε_{sav} = volume fraction of the solids in the cake
μ = filtrate viscosity, Pa.s
μ = viscosity of the filtrate, cp
ρ_L = density of drilling fluid, kg/m^3
ρ_s = density of solids, kg/m^3
ϕ_s = volume fraction of the solids in the drilling fluid
ϕ_c = porosity of the filter cake, volume fraction
ϕ_f = final porosity of ceramic disk after filtration process, volume fraction
ϕ_i = initial porosity of ceramic disk, volume fraction

Acknowledgment

The authors would like to thank the Saudi Arabian Oil Company for funding this project and Kate Brady for proofreading this paper.

References

Al-Abduwani, F.A.H., Bedrikovetsy, P., Farajzadeh, R., van den Broek, W., and Currie, P.K. 2005. External Filter Cake Erosion: Mathematical Model and Experimental Study. Paper SPE 94635 presented at the SPE European Formation Damage Conference, Sheveningen, The Netherlands, 25–27 May. http://dx.doi.org/10.2118/94635-MS.

Bourgoyne, A.T., Millheim, K.K., Chenevert, M.E., and Young, S.F. 1991. *Applied Drilling Engineering*, second (revised) printing, Vol. 2. Richardson, Texas: Textbook Series, SPE.

Civan, F. 1994. A Multi-Phase Mud Filtrate Invasion and Wellbore Filter Cake Formation Model. Paper SPE 28709 presented at the International Petroleum Conference and Exhibition of Mexico, Veracruz, Mexico, 10–13 October. http://dx.doi.org/10.2118/28709-MS.

Civan, F. 1996a. A Multi-Purpose Formation Damage Model. Paper SPE 31101 presented at the SPE Formation Damage Control Symposium, Lafayette, Louisiana, USA, 14–15 February.

Civan, F. 1996b. Interactions of the Horizontal Wellbore Hydraulics and Formation Damage. Paper SPE 35213 presented at the Permian Basin Oil and Gas Recovery Conference, Midland, Texas, USA, 27–29 March. http://dx.doi.org/10.2118/35213-MS.

Civan, F. 1998. Practical model for compressive cake filtration including fine particle invasion. *AIChE J.* **44** (11): 2388–2398. http://dx.doi.org/10.1002/aic.690441107.

Jiao, D. and Sharma, M.M. 1994. Mechanism of Cake Buildup in Crossflow Filtration of Colloidal Suspensions. *J. Colloid Interface Sci.* **162** (2): 454–462. http://dx.doi.org/10.1006/jcis.1994.1060.

Khatib, Z.I. 1994. Prediction of Formation Damage Due to Suspended Solids: Modeling Approach of Filter Cake Buildup in Injectors. Paper SPE 28488 presented at the SPE Annual Technical Conference and Exhibition, New Orleans, 25–28 September. http://dx.doi.org/10.2118/28488-MS.

Lambert, M.E. 1981. A Statistical Study of Reservoir Heterogeneity. MS thesis, University of Texas at Austin, Austin, Texas, USA.

Li, W., Kiser, C., and Richard, Q. 2005. Development of A Filter Cake Permeability Test Methodology. Paper presented at the American Filtration & Separations Society 2005 International Topical Conferences & Exposition, Ann Arbor, Michigan, USA, 19–22 September.

Martinez, M.Y., Mayne, M.D., Ortega, J.D., Trujillo, C., and Maestas, A. 2000. The Advantages of Using a Multiple Leaf Filter System in a Chloride Separations Process. Society of Mexican American Engineers and Scientists International Symposium and Career Fair, Santa Clara, California, USA, 19–23 January.

Osisanya, S.O. and Griffith, J. 1997. Evaluation of Cement Slurry Quality Using Filter Cake Permeability And Thickness. Paper PETSOC 97-136 presented at the Annual Technical Meeting, Calgary, Alberta, 8–11 June. http://dx.doi.org/10.2118/97-136.

Rautela, M.S. 2000. A Method for Determination of the Permeability of the Filter Cake at Wellsite. Paper SPE 50692 available from SPE, Richardson, Texas.

Tien, C., Bai, R., and Ramarao, B.V. 1997. Analysis of cake growth in cake filtration: Effect of fine particle retention. *AIChE J.* **43** (1): 33–44. http://dx.doi.org/10.1002/aic.690430106.

Tiller, F.M. 1990. Tutorial: Interpretation of filtration data, I. *Fluid/Part. Sep. J.* **3** (1): 85–94.

Tiller, F.M. 2002. *Theory and Practice of Solid-Liquid Separation*, fourth edition. Houston, Texas: University of Houston.

Salaheldin Mahmoud Elkatatny is a research assistant with Texas A &M University. His areas of interest include filter-cake characterization and removal. Elkatatny has published five conference papers for various SPE conferences. He holds BSc and MSc degrees from Cairo University, Egypt, and he is currently a PhD student in Texas A&M University in petroleum engineering.

Mohamed Ahmed Nasr Eldin Mahmoud is an assistant professor in the Department of Petroleum Engineering at FFUPM, KSA. His area of research includes carbonate and sandstone stimulation, formation-damage removal from sandstone reservoirs, and drilling-fluid filter-cake characterization. Mahmoud has published 28 conference papers and six journal publications, all in petroleum engineering. He holds BSc and MSc degrees from Suez Canal University, Egypt, and a PhD degree from Texas A&M University, all in petroleum engineering.

Hisham A. Nasr-El-Din is a professor and holder of the John Edgar Holt Chair in Petroleum Engineering at Texas A&M University. Previously, he worked for 15 years as Principal Professional and Team Leader of the Stimulation Research and Technology Team, Saudi Aramco. Before joining Saudi Aramco, he worked for 4 years as a staff research engineer with the Petroleum Recovery Institute in Calgary. He also worked as a research associate with the University of Saskatchewan, the University of Ottawa, and the University of Alberta. Nasr-El-Din's research interests include well stimulation, formation damage, cementing, drilling fluids, two-phase flow, enhanced oil recovery, rheology, conformance control, interfacial properties, adsorption, and nondamaging fluid technologies. Nasr-El-Din holds several patents and has published more than 480 technical papers. He has received numerous awards within Saudi Aramco for significant contributions in stimulation and treatment-fluid technologies and stimulation design, and for his work in training and mentoring. Nasr-El-Din holds BS and MS degrees from Cairo University and a PhD degree from the University of Saskatchewan, all in chemical engineering. He serves on the SPE steering committees on corrosion and oilfield chemistry, is an Associate Editor for *SPE Journal* (*SPEJ*) and is a reviewer for *SPE Production & Operations* (*SPEPO*) and *SPE Drilling & Completion*. He received the SPE Regional Technical Discipline Award for Production and Operations in 2006, was named a Distinguished SPE Member in 2007, and received SPE awards for Outstanding Associate Editor (*SPEJ*) and Outstanding Technical Editor (*SPEPO*) in 2008. In addition, he received the 2009 SPE Production and Operations Award and the 2009 Outstanding Associate Editor Award (*SPEJ*).